Arkadiusz Szarek*, Piotr Paszta**

Possibilities of the Manufacturing and Simulation of the Load on a Customised Mouthguard Used in Combat Sports

DOI: 10.5604/01.3001.0013.7324

Czestochowa University of Technology, Faculty of Mechanical Engineering and Computer Science, Institute of Mechanical Technologies,
Al. Armii Krajowej 21, 42-201 Częstochowa, Poland,
* e-mail: arek@iop.pcz.pl,
** e-mail: paszta@itm.pcz.pl

Abstract
The article presents an assessment of the state of stress and deformation of a personalised tooth protector, taking into account various types of elastomer materials that allow optimal protection of the teeth in contact combat sports. The load characteristics of the personalised protector, perfectly adhering to all, even clearly protruding from the anatomical line of teeth, were calculated using ANSYS 18 software. Numerical simulations of different elastomer materials were compared. Assessment of the state of stress and deformation of the protector allowed to demonstrate the legitimacy of protecting teeth with a personalised tooth protector and to increase the safety of the teeth and soft tissues of the oral cavity in contact combat sports. Based on a dental impression and plaster casting of the jaw made using an eviXscan 3D scanner, its model was digitalised. CAx techniques were used to design a mouthguard. Furthermore, a control code was generated and transmitted to a CNC milling machine to make a mouthguard fitted to the user's teeth.

Key words: *customized mouthguard, finite element method, CNC, hyperelasticity.*

Introduction

Injuries to teeth occur very often following various accidents. The highest risk of injury is most common in sport and due to unfortunate events. The oral cavity is heavily vascularised, and the rapid contact of soft tissues with teeth or a direct impact on the vascularized structures cause intense bleeding.

Due to elevated adrenaline levels, some injuries are initially imperceptible, and there are those that can only be diagnosed by specialists and radiological examinations. The consequences of an injury can be experienced after a long time has elapsed since it occurred. Injuries often lead to the dislocations or chipping of teeth and to the fracture of the lower jaw. Athletes with malocclusions, such as teeth protrusion, are particularly at risk.

With their specific structure, elastomer mouthguards are deformed under external forces and return to their original shape when the force is relieved, which consequently leads to impact damping. In the case of malocclusion or protrusions, the risk of injury to the front upper teeth is increased and injuries often occur to the soft tissue surrounding the teeth as well as face and head injuries. In some sports, blows are inflicted with fists, heels and knees to the head, which increases the risk of injuries not only to teeth but also to the brain and cervical spine.

The concept of a mouthguard was introduced when injuries during boxing matches became common. Initially, boxers used cotton, sponge or softwood sticks to protect their mouths and teeth, which they had to squeeze between their teeth [1].

The mouthguard is a simple elastic structure made of flexible, gutter-shaped plastic that fits both upper and lower teeth. This device is held in the mouth by the user to reduce his or her risk of injury, especially injuries to the teeth, gums and cheeks, caused by events occurring during his or her sporting activity. In most cases, mouthguards fully cover only the upper teeth. Sometimes double mouthguards are used to protect the lower teeth and gums, as well as dental braces, but in practice they are considered uncomfortable and significantly limit proper ventilation during activity.

The simplest mouthguards represent the cheapest way to protect the athlete and are available in sports goods stores. Formed in the shape of an arch-curved gutter made in many sizes, they are ready to be immediately put on after purchase. It is impossible to modify their shape in any way. Sometimes they can be corrected by cutting with a knife. Their only advantage is the very low price and easy access, and they have many disadvantages, such as the lack of fit, resulting in an uneven load distribution, substantial play, and they are held onto teeth only by clenching, which can cause abrasions and minor injuries to gums. They cause the accumulation of loads to individual teeth without tying them together. Most

Szarek A, Paszta P. Possibilities of the Manufacturing and Simulation of the Load on a Customised Mouthguard Used in Combat Sports.
FIBRES & TEXTILES in Eastern Europe 2020; 28, 2(140): 110-118. **DOI:** 10.5604/01.3001.0013.7324

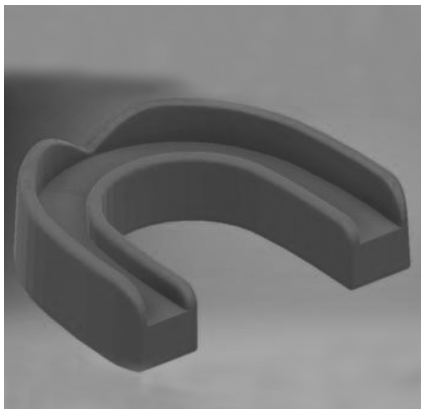

Figure 1. *Universal blank of the mouthguard.*

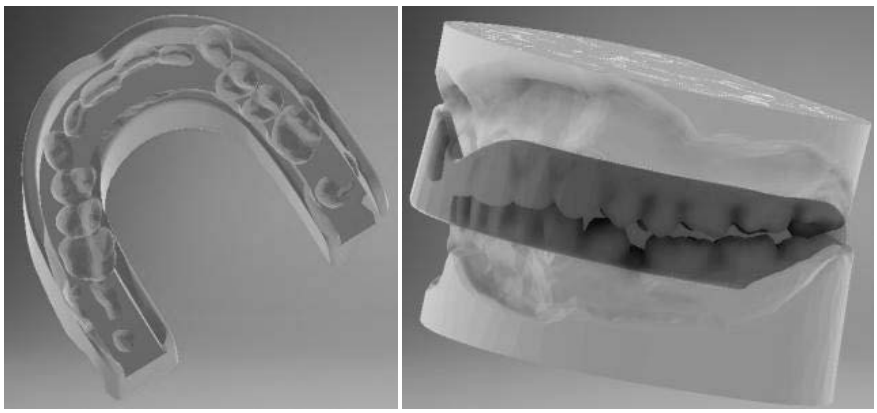

Figure 2. *Moulded mouthguard model.*

often they are made of polyvinyl chloride. Most dentists do not recommend their use.

Mouthguards made of thermoplastic materials are also called 'boil and bite'. They are also generally available in a precast form in basic sizes. The user puts it into the mouth after it has been heated in hot water and models the mouthguard by clamping the teeth and pressing with the fingers. They fit the teeth better than a non-mouldable mouthguard, can be heated several times, and formed again. Undoubtedly, their advantage is the price and availability in stores with equipment for combat sports. The disadvantages are a loose and imprecise fit and low occlusal force. There is also no proper distribution of forces on the adjacent teeth, and these mouthguards only absorb impacts. Moreover, they do not protect the gums and do not fully cover the area exposed to mouth injuries. If used for a longer period of time, they will loosen and harden over time. There are versions with a stiffer outer layer made of polyvinyl chloride, mouldable silicone rubber or acrylic gel.

The custom-made mouthguard fits very well and is comfortable to use due to its design being adjusted to the individual user. It gives the option to choose a model depending on the sport, the level of advancement of the player, and individual experiences and preferences. The disadvantages are the estimated 20 times higher manufacturing costs compared to mouldable mouthguards and the long time of waiting for manufacturing. The custom-made mouthguard is made from an anatomical impression so that it can fit the user's teeth precisely. Custom-made mouthguards are designed in a dental office under the guidance of a dentist and made by a technician in a dental laboratory. Two manufacturing methods are popular: vacuum forming and pressure lamination [2-5].

The protection of teeth is a significant problem, and currently used protectors do not sufficiently protect teeth and soft tissues from injury. The most commonly used protectors are made in series with an average anatomical shape of the jaws, and allow adaptation to the shape of the teeth under the influence of hot water (contraction after cooling). In both cases, it is not possible to obtain a protector that fits evenly to the surface of all teeth.

An additional problem is the selection of an optimal material that absorbs the loads resulting from an impact, while allowing the transfer and distribution of the force over an optimally large surface to minimise the destructive effects of the blow.

Method of manufacturing of a custom-made mouthguard

A custom-made mouthguard was designed to suit the individual needs of a person with the protrusion of the front teeth. The mouthguard design should provide adherence to all teeth and optimal transmission of punching forces, as well as prevent injuries to the face and teeth.

Anatomical impressions of the oral cavity were made. Impressions of the upper and lower teeth were scanned separately. An accurate impression scan was also performed at the maximum occlusion of the teeth in order to anatomically combine a plaster model of the dental system. The upper and lower teeth model was transferred to an Autodesk Inventor program. The distance was anatomically created, and the teeth were opened to create a space for the mouthguard. A spatial model, a universal blank of the mouthguard, with appropriate dimensions was previously prepared, as shown in ***Figure 1***.

The dimensional adjustment of the blank to dental arches was performed using the numerical method. Then the teeth in the mouthguard were impressed numerically, which allowed the mouthguard to perfectly fit the bite. There is a possibility of multiple adjustments of different types and thicknesses of the blank, as well as changing the distance of the teeth and depth of bite. Adjustment of the mouthguard geometry is virtually unlimited. The method proposed offers opportunities to design mouthguards for athletes with an atypical anatomical structure of teeth or for those undergoing orthodontic treatment. The mouthguard is usually used for a relatively short period of time or only once. The method proposed makes it possible to manufacture a perfectly fit mouthguard that ensures great comfort of use and is held in the right position. The mouthguard covers teeth and jawbone parts. It can also reduce the risk of concussion in the event of a severe blow to the jaw, which can produce a pressure wave and cause concussion injury. ***Figure 2*** shows a model of a ready-made mouthguard designed for a specific user.

Punch force

Performing strong punches depends on a technique that involves the entire body. The muscles of the legs, abdomen and lower back are essential for a strong punch, as are the muscles of the lower back, whereas the muscles of the hand act only additionally. A blow to the head can lead to a jaw injury, concussion and

changes in the position of the brain inside the skull.

A comprehensive study of the results of boxing fights, types of punches and measurement of their strength and speed were presented in paper [6]. Scientific research revealed that most of the speeds ranged from 4.5 m/s to 15.5 m/s. Punches at a speed of 21 m/s occur exceptionally. Rear punches are typically faster than lead punches, and hook punches are typically faster than straight punches, with more advanced fighters typically faster than newer ones.

Measurements of forces under experimental conditions were in the range of 1100 N to 4900 N. There is a large disproportion between forces measured experimentally and those a real fight in the ring.

The average person who has not previously practised boxing performs punches which are about ten times weaker than a professional [7]. The FEM analysis adopted impact forces based on literature analysis and own experience in combat sports.

Analysis of material models

Rubber and rubber-derived materials are elastomers composed of long aliphatic polymeric chains that were cross-linked in the process of vulcanization and have specific physical and chemical properties. If forces are applied, the Mullins and Payne effects are observed, and these materials are often modelled as hyperelastic. The name rubber is commonly used for many elastomers. With the ease of use and low cost, rubber has been widely used in medicine, the automotive industry, and in other sectors due to its strength, durability and deformation capability of up to 700% without damage. Elastomers show complex mechanical behaviour that does not fit into the application of linear elasticity theory. The mechanical properties of rubber are represented as a function of the strain energy balance. Many phenomenological theories have been developed to define the behaviour of elastomers, which causes complications with regard to modelling elastomers compared to other engineering materials for which Hooke's law can be applied.

Elastomers can be defined by the stored energy function as hyperelastic. The coefficients in these functions should be determined using experimental data from biaxial tension, compression and shear. The problem is to determine the function of the strain energy in dependence on the experimental data obtained.

With a slight strain of up to several percent, rubber exhibits the characteristics of a linearly elastic material, like other solids, and in this respect, it is acceptable to use such a solution in engineering problems. However, above this range, a non-linear shape of the stress-strain curve is observed, which means that the strain is not directly proportional to the force applied.

According to the phenomenological Rivlin theory, rubber is accepted as a material which is isotropic in terms of elasticity and almost incompressible. For rubber modelling, constitutive models based on polynomials describing the balance of strain energy are used. Most of the models are based on strain invariants I_1, I_2, I_3.

$W = f(I_1, I_2, I_2)$ where: $I_1 = \lambda_1^2 + \lambda_2^2 + + \lambda_3^2$, $I_2 = \lambda_1^2\lambda_2^2 + \lambda_2^2\lambda_3^2$, $I_3 = \lambda_1^2\lambda_2^2\lambda_3^2$, $\lambda_1, \lambda_2, \lambda_2$ – tension coefficients for the directions of the coordinate system. According to equation:

$$W = \sum_{i+j+k}^{\infty} C_{ijk} (I_1 - 3)^i (I_2 - 3)^j (I_{3-1})^k$$

The phenomenological model of strain of incompressible hyperelastic materials for $I_3 = 1$ is:

$$W = \sum_{i+j}^{\infty} C_{ij} (I_1 - 3)^i (I_2 - 3)^j.$$

The most famous of these are the models developed by Ogden, Mooney-Rivlin, Neo-Hookean, Arruda-Boyce, and Yeoh. The range of strains and definition of constants of polynomials based on laboratory tests are critical. The Mooney-Rivlin model provides good mapping in a range of up to 300% strain.

The Ogden material model shows a strain energy function based on the principal stretches $\lambda_1, \lambda_2, \lambda_2$ for incompressible materials $\lambda_1, \lambda_2, \lambda_2 = 1$. Coefficients for the directions of the coordinate system axes can be measured, which represents an advantage of this model. The elastic energy function defined by Ogden is represented by equation:

$$W = \sum_i^N \frac{2\mu_1}{\alpha_i^2}\left(\lambda_1^{\alpha_i} + \lambda_2^{\alpha_i} + \lambda_3^{\alpha_i} - 3\right) + + \sum_i^N \frac{1}{D_i}(J_{el} - 1)^{2i},$$ where $\lambda_i = J^{\frac{-1}{3}}\lambda_i$, $J = \lambda_1\lambda_2\lambda_3$,

λ_i the principal stretches, J the Jacobean determinant, and J_{en} the elastic volume ratio. Constants μ_1 and α_i describe the shear behaviour of the material and the D_i compressibility. If data from many experiments are available, the Ogden model will be well matched to the material and accurate.

The Mooney-Rivlin material model is popular for incompressible elastomeric materials. It is a special case, being the result of the general form of the elastic energy function defined by Rivlin and Saunders and proposed by Mooney as the empirical form of the strain energy function.

This model is defined by the following equation:

$$W = \sum_{ij}^N C_{ij} (I_1 - 3)^i (I_2 - 3)^j + + \sum_i^N \frac{1}{D_i}(J_{el} - 1)^{2i},$$ where $C_{00} = 0$, C_{ij} are material parameters, and D is the material incompressibility parameter.

The strain energy function for the 2-parameter model is:

$$W = C_{10}(I_1 - 3) + C_{01}(I_2 - 3) + + \frac{1}{D}(J - 1)^2, \mu = 2(C_{10} + C_{01}).$$

Neo-Hookean model. The form of the Neo-Hookean strain-energy potential is:

$$W = \frac{\mu}{2}(I_1 - 3) + \frac{1}{D}(J - 1)^2,$$

where: μ – initial shear modulus of the materials, and D – the material incompressibility parameter. The initial bulk modulus is related to the material incompressibility parameter by $K = \frac{2}{D}$, where: K – initial bulk modulus.

In the case of large strains, each rubber-based material behaves in a different manner. It has not yet been possible to propose a generalised constitutive relationship and examinations are needed for individual materials. The disadvantages of the models presented include the necessity of multiple experimental tests and complications related to calculations with a large number of parameters [8-11].

Explicit dynamics simulation in ANSYS

Finite element simulation requires access to software to import or execute an object geometry model, divide it into finite elements in an appropriate way, define a material model, and provide boundary conditions as loads and restraints.

Table 1. *Uniaxial test data.*

Strain, m m^{-1}	Stress, Pa
0.1338	10691.01486
0.2675	16800.46169
0.3567	21382.71919
0.6242	29019.35536
0.8917	36655.99154
1.1592	41237.55956
1.4268	47347.0064
2.051	61093.08941
2.586	73311.2936
3.0318	85530.18728
4.3694	137458.7617
4.8153	161895.8596
5.172	189388.0256
5.4395	213825.1235
5.9299	264226.5085
6.0637	290190.7957
6.3312	340592.1808
6.465	366557.1575
6.5541	392521.4447

Table 2. *Biaxial test data.*

Strain, m m^{-1}	Stress, Pa
0.02	6470.042784
0.06	10962.6684
0.11	16607.40841
0.14	18078.06072
0.2	22918.18224
0.31	30528.61833
0.42	35735.54108
0.68	45521.96342
0.94	53637.09594
1.49	67470.05293
2.03	87115.98208
2.43	101217.8347
2.75	119968.824
3.07	138624.6656
3.26	154788.741
3.45	169976.5183

Table 3. *Shear test data.*

Strain, m m^{-1}	Stress, Pa
0.1034	11031.616
0.1724	16547.424
0.2828	23166.3936
0.4276	28957.992
0.8483	41368.56
1.3862	53779.128
2.0	66189.696
2.4897	76669.7312
3.0345	89356.0896
3.4483	102594.0288

Table 4. *Volumetric test data.*

Volume ratio	Hydrostatic pressure, Pa
0.8847	1593379.036
0.9127	1207961.952
0.9412	814960.632
0.9703	413685.6

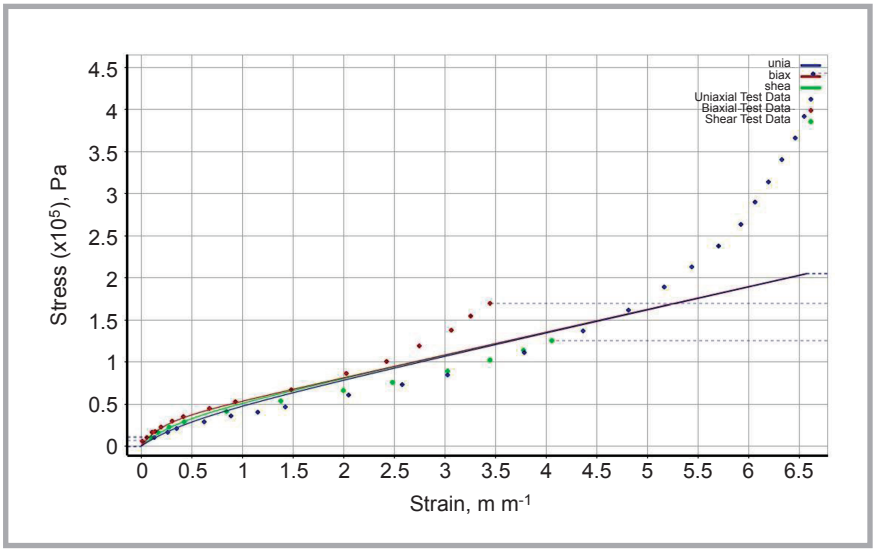

Figure 3. *Adjustment of curves to the Neo-Hookean model.*

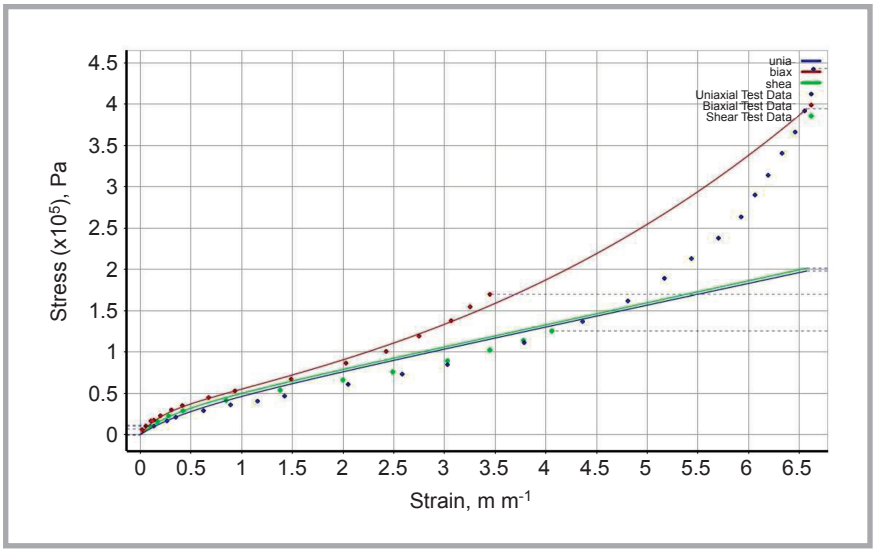

Figure 4. *Adjustment of curves to the Mooney-Rivlin 2 parameter.*

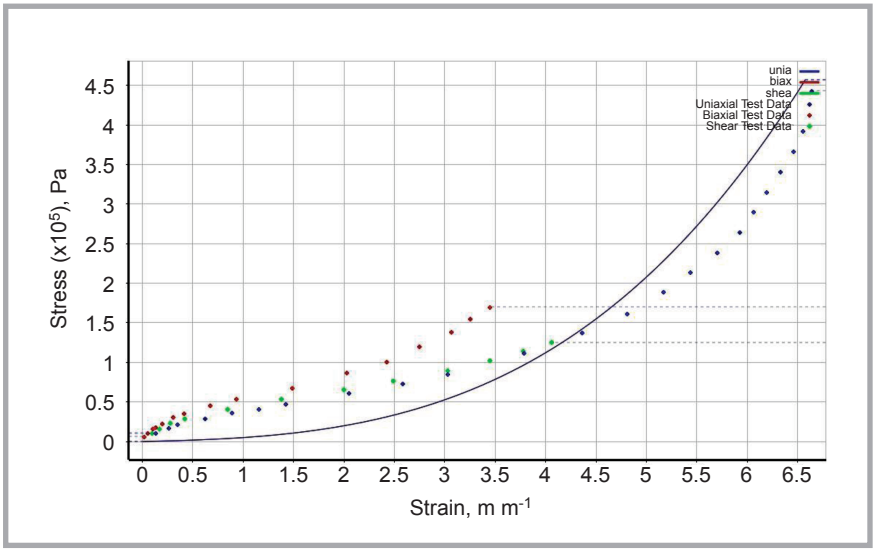

Figure 5. *Adjustment of curves to the Ogden 3rd order model.*

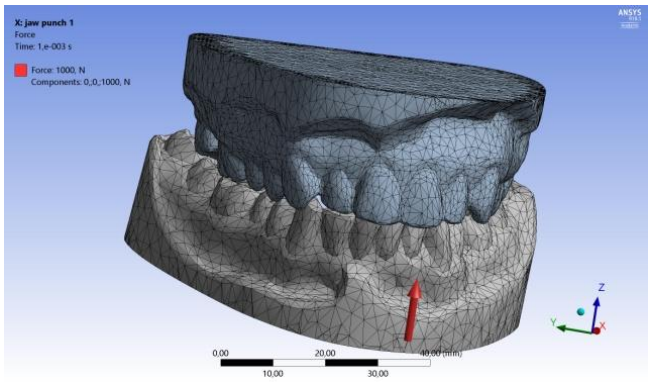

Figure 6. *3D model with force load.*

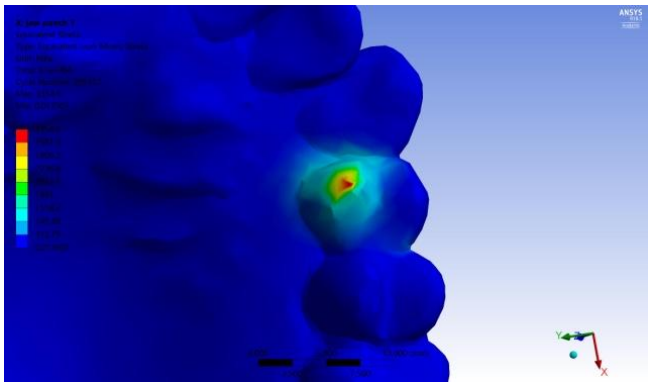

Figure 7. *Point stresses of the cusps of a tooth at 3354 MPa.*

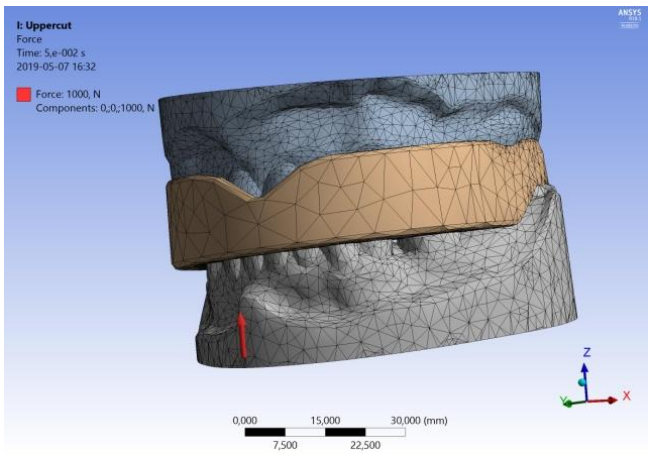

Figure 8. *3D model loaded with a force of 1000 N, case 1.*

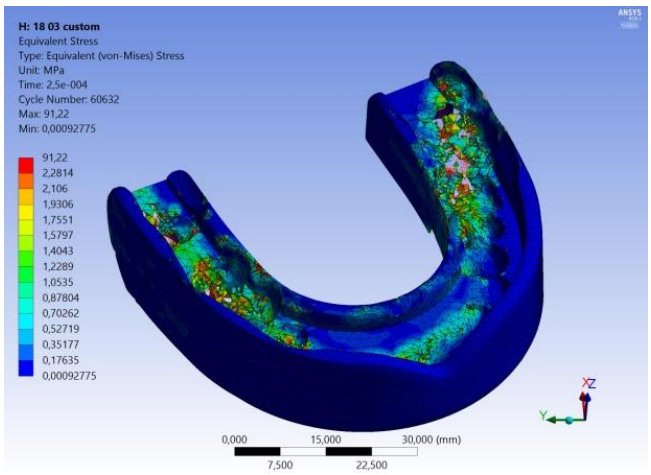

Figure 9. *Von Mises stress distribution in the mouthguard, case 1.*

ANSYS is the world's largest manufacturer of computer simulation software based on finite element and finite volume methods and has the most advanced numerical analysis tools available in the market. All ANSYS modules are contained in the ANSYS Workbench platform [12].

Under laboratory conditions, elastomer characterisation is obtained by single-axis tensile testing, which is standardised [13]. In the biaxial tensile test, which captures the behaviour of materials under a multidirectional load, which is closer to the actual operating conditions, the solutions proposed suggest using synchronised motors working in two axes simultaneously or special holders mounted on the testing machine. An example of biaxial tensile testing and analysis is in study [14]. Additional coefficients of polynomial equations are obtained from hydrostatic compression tests or pure shear tests.

The experimental results obtained are used to determine the coefficients of equations by adjusting the measurement curves to the regression curves resulting from the material models proposed. Users should check the applicability of the model selected before using it.

ANSYS 18 software on the PIONIER platform [15] was used to present material data and their adjustment to the material models by Ogden, Mooney Rivlin and Neo Hooken. ***Tables 1-4*** present experimental data of the single and biaxial stretching and shear and hydrostatic compression of neoprene rubber [16, 17].

Figure 3-9 show a match between experimental data and the material models by Ogden, Mooney Rivlin and Neo Hooken. Choosing the best material law can be a difficult trial and error process.

Two material models of rubber were adapted in the analysis. The Ogden model: density 1000 kg/m^3, material constant MU1 = 6.1803*10^5 Pa, material constant A1 = 1.3, material constant MU2 = 1180 Pa, material constant A2 = 5, material constant MU3 = -9810 Pa, material constant A3 = -2, incompressibility parameter D1 = 4.825*10^{-9} Pa^{-1}, incompressibility parameter D2 = 0 Pa^{-1}, and incompressibility parameter D3 = 0 Pa^{-1}.

The Mooney-Rivlin model: density 1000 kg/m^3, material constant C10 = 1.5*10^5 Pa, material constant C01 = 15000 Pa, and incompressibility parameter D1 = 1.212*10^{-9} Pa^{-1}. For neoprene rubber and the data presented in the tables, the coefficients of the Neo-Hookean model are as follows: initial shear modulus MU = 27104 Pa, and incompressibility parameter D1 = 1.4429*10^{-7} Pa^{-1}. Mooney-Rivlin model coefficients: material constant C10 = 13080 Pa, material constant C01 = 226.01 Pa, and incompressibility parameter D1 = 1.4429P10-7 Pa^{-1}. The Ogden model coefficients: material constant MU1 = 162.5 Pa, material constant A1 = 4.3725, material constant MU2 = 162.5, material constant A2 = 4.391, material constant MU3 = 162.5 Pa, material constant A3 = 4.37431, incompressibility parameter D1 = 1.4346*10^{-7} Pa^{-1}, incompressibility parameter D2 = 1.7474*10^{-7} Pa^{-1},

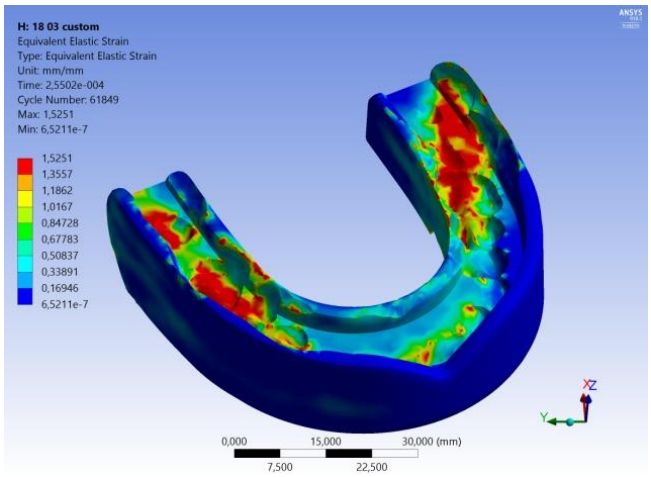

Figure 10. *Distribution of strains in the mouthguard, case 1.*

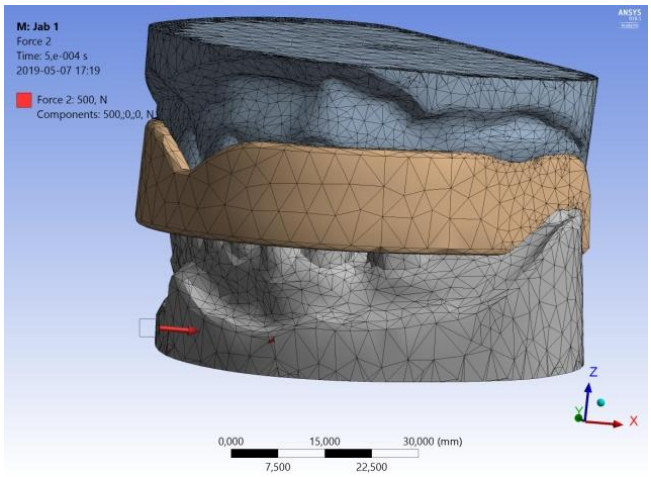

Figure 11. *3D model loaded with a force of 500N, case 2.*

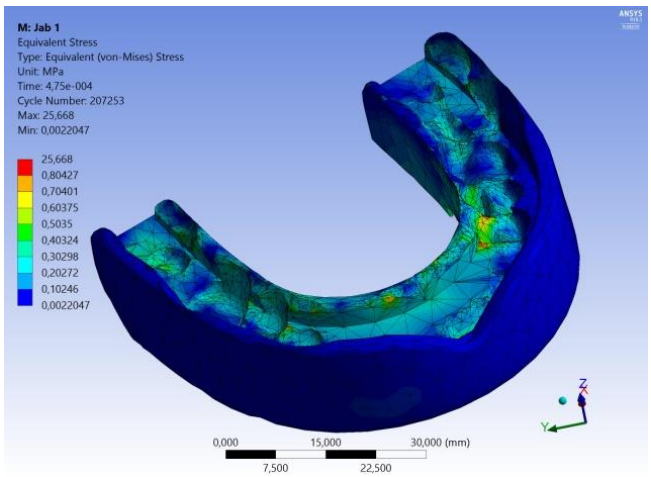

Figure 12. *Von Mises stress distribution in the mouthguard, case 2.*

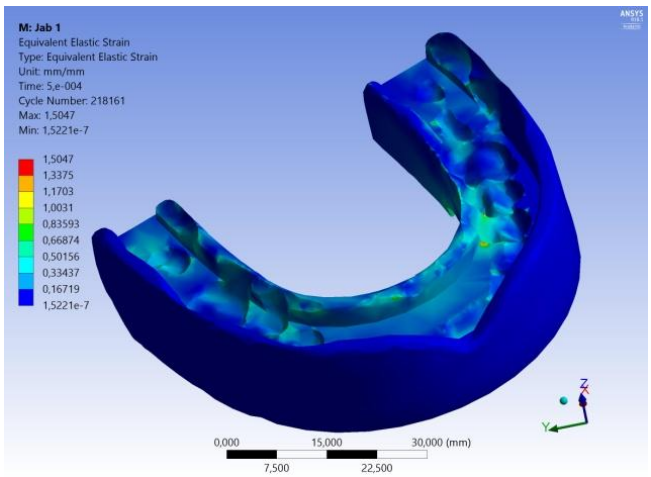

Figure 13. *Distribution of strains in the mouthguard, case 2.*

and incompressibility parameter D3 = 5.7345*10^{-9} Pa^{-1} [18].

ANSYS Workbench 18 software was used in combination with Autodesk Inventor to simulate the behaviour of the jaw impression in contact with the mouthguard under dynamic load conditions. The Solwer AUTODYN program was used to generate analysis results. The analysis was performed using a scanned model of jaws with teeth that reflects the actual conditions. The non-linear analysis shows a model with and without a mouthguard for different elastomeric materials. The model that was made in the Inventor program is composed of three parts and was imported into ANSYS Workbench 18 in .iam format.

Material properties of the components are described above. A mesh with tetrahedron elements was generated to suit the modelling of complex irregular models such as jaw impressions. To apply a specific force, it is necessary to specify the value, direction, and sense of the force, and select the geometry to which it is applied. The jaws were restrained and a force of a certain value was applied to the lower jaw in the direction selected. Maps of reduced von Mises stresses and strains were obtained.

The criterion used to evaluate the strength of a material at complex stress conditions is the modified von Mises criterion. Results of the calculations are presented in the form of stress maps.

Figure 6 shows the assumed boundary conditions of the model, while ***Figure 7*** depicts the simulation of a change in the stress distribution in the teeth after an impact to the jaw by a punch to the chin with a force of 1000 N applied in the incisal direction of the lower teeth at a speed of 15 m/s. The analysis shows the concentration of stress on the crowns of incisors increases in the direction of the molars, amounting to 3354 MPa. The characteristic feature is the impact of the lower jaw against the upper jaw and its rebound. Analysis of the response of the system to the impact and concentration of the stress fields on the teeth reveals a tendency for stresses to concentrate on the cusps of teeth, which causes the chipping of individual teeth. A similar situation occurs during the analysis of changes in the strain fields.

A dynamic simulation was presented for the following cases:

1. Punch to the chin, impact force: 1000N, speed: 15 m/s, Mooney-Rivlin model mouthguard material.
2. The results are presented in ***Figures 8*** to ***10***. There are visible stresses in the mouthguard in the area of molar teeth, causing the mouthguard to lose its integrity.
3. Straight punch, impact force: 500 N, speed: 15 m/s, jaw clamping force: 50 N, Ogden model mouthguard material.

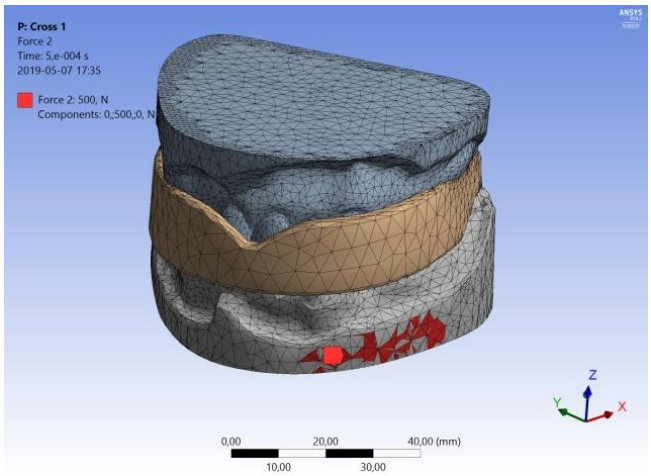

Figure 14. *3D model loaded with a force of 500N, case 3.*

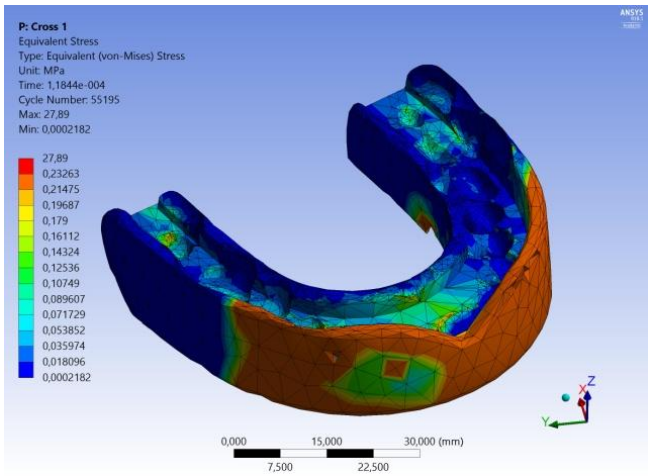

Figure 15. *Von Mises stress distribution in the mouthguard, case 3*

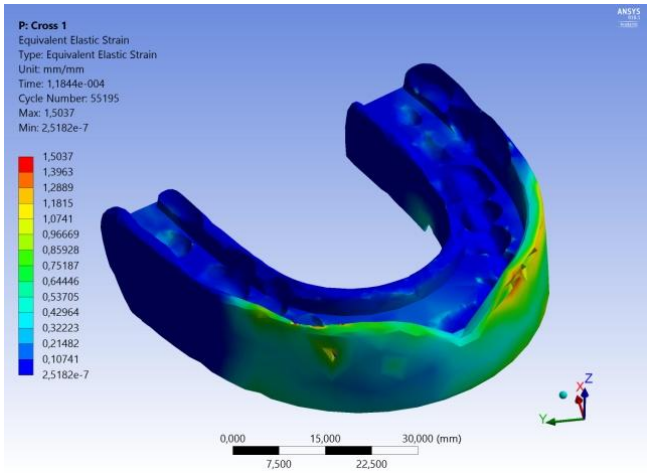

Figure 16. *Distribution of strains in the mouthguard, case 3.*

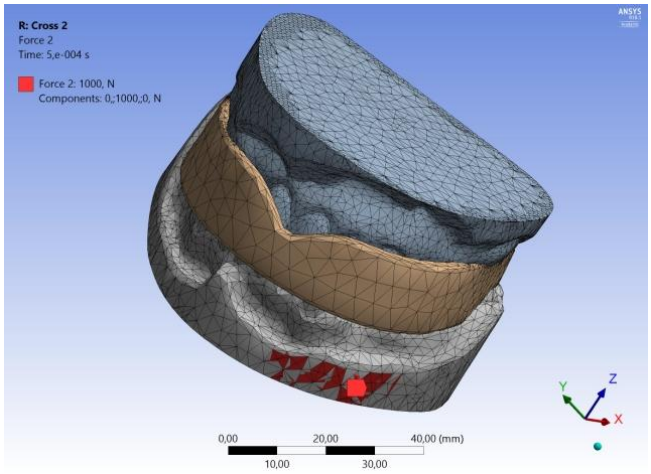

Figure 17. *3D model loaded with a force of 1.000 N, case 4.*

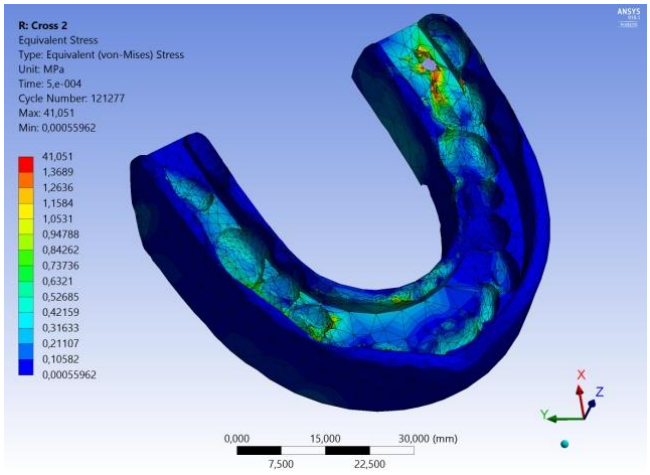

Figure 18. *Von Mises stress distribution in the mouthguard, case 4.*

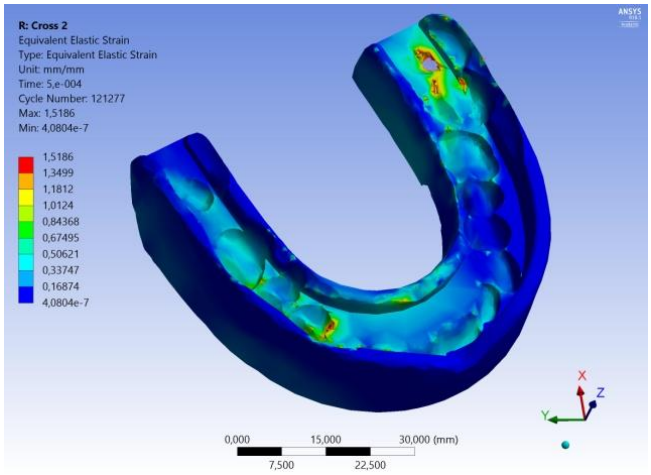

Figure 19. *Distribution of strains in the mouthguard, case 4.*

4. The results are presented in ***Figures 1*** to ***13***. A strong bite of the mouthguard between the cusps of the right molar teeth is observed, with a tendency to lose material consistency.

Side impact force: 500 N, speed: 15 m/s, jaw clamping force: 30 N, Mooney-Rivlin mouthguard model material. The results are presented in ***Figures 14*** to ***16***. Due to the type of impact, the load is taken over by the front part of the mouthguard. Low reduced stresses of 0.23 MPa.

Side punch, impact force: 1000 N, speed: 15 m/s, jaw clamping force: 50 N, Ogden

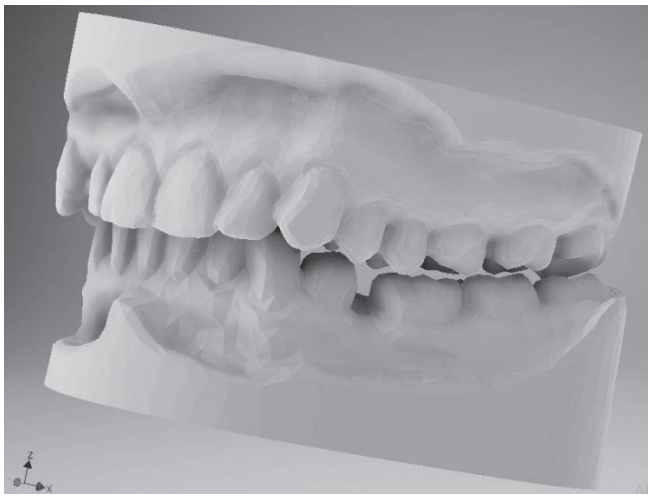

Figure 20. *Results of scanning and processing of the impression.*

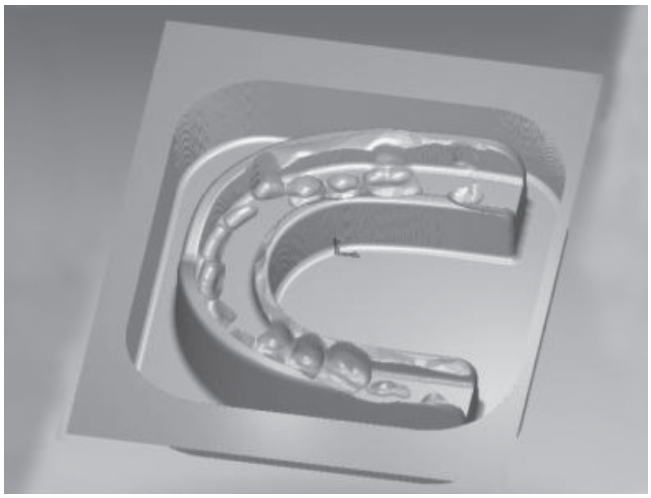

Figure 21. *Result of the simulation of the manufacturing of mouthguard components.*

model mouthguard material. The results are presented in ***Figures 17*** to ***19***. A tendency to bite the mouthguard with molar teeth can be observed.

The numerical tests allowed for the development and implementation of a protector taking into account the individual protrusion of anterior teeth and molar tooth defects. Numerical analysis of the model, taking into account the various materials of the protector, allowed the fitting and optimisation of the element both in terms of the shape and allocation of teeth and the selection of material that optimally moves the opponent's blows.

Scanning

A point cloud is obtained when mapping an object, representing the scanned object. It provides the basis for further processing. Creating a proper model as a result of the digitalisation process is not an easy task as it requires much time and professional equipment.

Spatial scanning is based on a technique that makes it possible to optically measure the spatial coordinates of a point. The eviXscan 3D Loupe + scanner, designed by Polish engineers, is a mobile and universal object scanner used in reverse engineering. This scanner is utilised in the case of objects which require particularly high resolution.

Its design makes it possible to scan very small objects with all their special characteristics, such as sharp edges. It is characterised by high precision, with a scanning accuracy of 0.02 mm, according to DE VDI/VDE2634. The scanner allows users to process point clouds into a triangle grid and export data to .asc, .bin, .stl, .ply and .obj files. The principle of the 3D scanner operation is based on emitting white stripes to the scanned object using an installed projector and analysis of the deviations of stripes displayed on the object examined.

Several series of scans were performed to obtain three solids: the upper jaw, lower jaw, and with clenched teeth. The scanner projector's light does not reach the cavity, resulting in no cloud points in this place, no forming of a surface, and the necessity of repeating scans. The point cloud obtained had to be cleaned off excess points created by other objects in the vicinity of the scanned object. In order to create one model (one grid of triangles) from several scans, software designated by the scanner manufacturer (Leios 2) was used, allowing for trouble-free work on data obtained from 3D scanning. It enables to obtain an advanced edition of point clouds and triangle grids, as well as basic reverse engineering tasks. Furthermore, it enables the basic verification of components by comparing them with the CAD model or other scanned objects. The program is capable of handling the entire scan processing, from the point cloud to parametric surfaces.

The triangle grid accurately reproduces the surface of the object, forming the basis for the creation of a CAD model and then technical documentation of the object. The final result of scanning and machining is shown in ***Figure 20***.

For further purposes, the object was exported to an STL file, which can be opened in Autodesk Inventor. In this program, the MeshEnabler tool was used to create solids from scanned elements. The ready-made jaw model was used to make an impression in the designed mouthguard [19, 20].

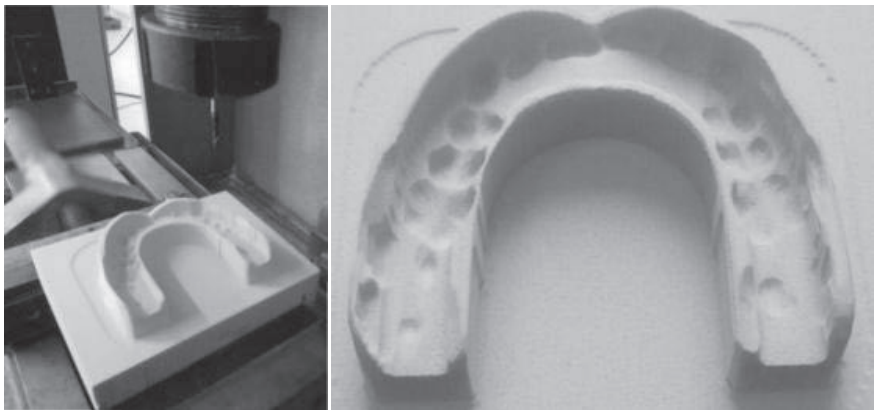

Figure 22. *Example of mouthguard surface machining using a CNC milling machine.*

Making the mouthguard

As an example of a manufacturing possibility, the mouthguard was made in lightweight polyurethane foam on a CNC FYS milling machine, and the manufacturing process and program code were prepared using the ArtCAM program. ArtCAM is a CAD/CAM program and a tool to support design and manufacturing. The object creation process is supported from model creation through planning of the machining process to the generation of an NC code, which, using many postprocessors, will be adapted to the machine control system.

It allows for the roughing and finishing of 3D models imported in the .stl format, simulating tool paths and checking the tool trajectory, and the machining effect can be known even before the actual manufacturing of the component. Machining can be performed by means of conventional three-axis or multi-axis milling machines. The program features a number of machining strategies that ensure quick and efficient work. The possibility to choose from a database of tools with the most common shapes, or to create customised tools, allows to obtain the surface finish desired.

Machining was performed using a ball engraving cutter. The next step in setting the machining parameters was to select the machining strategy. The setting process was performed using the offset method, climb milling method, and the internal starting point. The trajectory of the tool path was then generated. This simulation allows, among other things, to diagnose possible tool collisions, improve the machining strategy, eliminate unnecessary movements, and check the theoretical roughness of the surface after machining. ***Figure 21*** shows the result of simulation of mouthguard machining.

The next step was milling. The material was placed and fixed on a milling table. Using a universal 3D measurement sensor, the spindle of the machine tool was set on the axis of the workpiece, and the perpendicularity of the material face was measured.

After the tool was set, the code of the machining program was uploaded. The program was transmitted via serial port RS-232, using HyperTerminal software. With the tool set and the program uploaded to the machine tool, a control simulation was performed on the machine screen. Checking the program allows for diagnosis of whether the program has been correctly transmitted and whether all tool movements are consistent with previous simulations. Mouthguard machining is presented in ***Figure 22***.

Conclusions

Nowadays, elastomeric mouthguards are an essential means of protection in many sports. Mouthguards are designed to absorb and distribute the impact generated during sporting activity. Teeth can injure the lips, tongue and cheeks, and may be chipped in contact with each other; other potential injuries include concussion, facial bone fractures and injuries to the lower jaw joints. In order to design a good mouthguard, it is important to know the size of the mouth of the user. However, it is difficult to indicate a standard dimension for the human oral cavity, with its structure changing with time. Therefore, based on the dental impression and plaster casting of the jaw made using an eviXscan 3D scanner, its model was digitalised. CAx techniques were used to design a customised mouthguard. The method proposed offers the possibility to better fit the mouthguard to any material, ensures higher biocompatibility due to a lower residual monomer content, and eliminates the inconveniences of the generally used components made of thermoplastic materials and the mismatch due to material shrinkage.

Using ANSYS 18 software, an example of an unprotected impact with a stress of 3354 MPa was also presented, leading to damage to the teeth, and a load on the custom-fit mouthguard, with blows performed from different directions to the lower jaw with a force of up to 1000 N at a speed of 15 m/s.

Selected phenomenological models describing the strain energy density for hyperelastic material were discussed. If properly defined, they allow to obtain the real state of stress, strain and preservation of the material.

The finite element method is an approximate solution that provides a reliable picture of the behaviour of conditions present in reality. The methods of generating and sending the control code to a CNC milling machine and the manufacturing of a customised mouthguard were also presented.

References

1. Knapik JJ, Marshall SW, Lee RB, Darakjy SS, Jones SB, Mitchener TA, Jones BH. Mouthguards in Sport Activities. *Sports Medicine* 2007; 37(2).
2. Pontsa P.T. Mouth Guards Prevent Dental Trauma in Sports. *The Dent-Liner* 2008; 12(3).
3. Patric DG, van Noort R, Found MS. Scale of protection and the various types of sports mouthguard. *Br J Sports Med* 2005; 39: 278-281.
4. Leffler W. Zastosowanie tworzyw polimerowych w zakresie ochrony jamy ustnej podczas uprawiania sportu. *Przetwórstwo Tworzyw* 2014; 20, nr 3 (159).
5. McCrory P. Do mouthguards prevent concussion? *British Journal of Sports Medicine* 2001; 35:81-82.
6. Langholz NJ. Pulling Punches: *A Non-parameteric Approach to Punch Force Estimation and the Development of Novel Boxing Metrics*. Dissertation University of California Los Angeles 2013.
7. https://ciekawe.org/2015/01/19/oblicza-boksu-w-trakcie-uderzenia
8. Ali A, Hosseini M, Sahari BB. A Review of Constitutive Models for Rubber-Like Materials. American *J. of Engineering and Applied Sciences* 2010; 3(1): 232-239.
9. Jaszczak P. Modelowanie gumy za pomocą metody elementów skończonych. *Elastomery* 2016; nr 3, t. 20.
10. Jensen A, Chee S. *Inverse Modelling of Material Parameters for Rubber-like material*. Liverpool John Moores University 2015.
11. Rackl M. *Curve Fitting for Ogden, Yeoh and Polynomial Models*. Ostbayerische Technische Hochschule 2015.
12. https://www.mesco.com.pl
13. PN-ISO 37:2007 Guma i kauczuk termoplastyczny, Oznaczanie właściwości wytrzymałościowych przy rozciąganiu.
14. Seibert H, Scheffer T, Diebels S. Biaxial testing of elastomers – Experimental setup, measurement and experimental optimisation of specimen's shape. Universitat des Saarlandes, *Technische Mechanik*, 2014; 34 (2): 72-89.
15. https://cloud.pionier.net.pl
16. Stamper E. *Determining Compressibility Properties for Hyperelastic FEA Models*. CAE ASSOCIATES 2014.
17. Ansys 18.2.2 Documentation.
18. Treloar LRG. Stress strain data for vulcanized rubber under various types of deformation. *Transactions of the Faraday Society*, 1944 vol. 40, pp. 59-70.
19. Paszta P. Digital possibilities of the reconstruction of machine parts. *MATEC Web of Conferences* 254, 01007 2019.
20. *Skaner evixscan 3D. Instrukcja użytkownika*. Evatronix 2016.

Received 19.10.2019 Reviewed 13.01.2020

Athens Institute for Education and Research

A World Association of Academics and Researchers

8th Annual International Conference on Industrial, Systems and Design Engineering, 22-25 June 2020, Athens, Greece

The Industrial Engineering Unit of ATINER will hold its **8th Annual International Conference on Industrial, Systems and Design Engineering, 22-25 June 2020, Athens, Greece** sponsored by the Athens Journal of Technology & Engineering.The aim of the conference is to bring together academics, researchers and professionals in areas of Industrial, Systems, Design Engineering and related subjects. You may participate as stream leader, presenter of one paper, chair of a session or observer. Please submit a proposal using the form available (https://www.atiner.gr/2020/FORM-IND.doc).

Important Dates

- Abstract Submission: **18 November 2020**
- Acceptance of Abstract: 4 Weeks after Submission
- Submission of Paper: **25 May 2020**

Academic Member Responsible for the Conference

- **Dr. Theodore Trafalis**, Director, Engineering & Architecture Division, ATINER, Professor of Industrial & Systems Engineering and Director, Optimization & Intelligent Systems Laboratory, The University of Oklahoma, USA.

Social and Educational Program

The Social Program Emphasizes the Educational Aspect of the Academic Meetings of Atiner.

- Greek Night Entertainment (This is the official dinner of the conference)
- Athens Sightseeing: Old and New-An Educational Urban Walk
- Social Dinner
- Mycenae Visit
- Exploration of the Aegean Islands
- Delphi Visit
- Ancient Corinth and Cape Sounion

More information can be found here: https://www.atiner.gr/social-program

Conference Fees

Conference fees vary from 400€ to 2000€
Details can be found at: https://www.atiner.gr/fees